[22]S. Sugano, Y. Tanabe, and H. Kamimura, *Multiplets of Transition-Metal Ions in Crystals* (Academic, New York, 1970).
[23]J. Kondo, Prog. Theor. Phys. **28**, 1026 (1962).
[24]W. H. Bauer, Acta Crystallogr. **11**, 488 (1958).

[25]J. W. Stout and S. A. Reed, J. Am. Chem. Soc. **5**, 5279 (1954).
[26]O. Schmitz-DuMont and H. Bornefeld, Z. Anorg. Allg. Chem. **287**, 120 (1956).

Pressure and Temperature Dependences of the Raman-Active Phonons in SnO_2[†]

P. S. Peercy and B. Morosin

Sandia Laboratories, Albuquerque, New Mexico 87115

(Received 25 September 1972)

The temperature (10–500 °K) and pressure (0–4 kbar) dependences of the four Raman-active phonons B_{1g}, E_g, A_{1g}, and B_{2g} as well as thermal expansion (93–700 °K) and isothermal compressibility (0–3 kbar) in SnO_2 were measured. These measurements allowed us to determine the mode Grüneisen parameters for the Raman-active phonons and to separate the isobaric temperature dependence of each frequency into pure-volume and pure-temperature contributions. By this procedure the cubic and quartic anharmonicities responsible for the pure-temperature contributions to the mode frequencies were determined. The B_{1g} mode in SnO_2 exhibited anomalous temperature and pressure dependences in that $\omega(B_{1g})$ increased with temperature and decreased with pressure. The remaining modes exhibited decreases in frequency with increasing temperature and increases in frequency with increasing pressure, characteristic of ionic crystals. The results are compared with the recent results on the isomorphic compound tetragonal TiO_2.

I. INTRODUCTION

Crystals of the rutile (TiO_2) structure comprise an important class of compounds. The tetragonal form of tin dioxide, SnO_2 (cassiterite), is the prototype structure for this class of materials. Because of the similarity of SnO_2 and TiO_2, various authors have compared their phonon frequencies using infared[1,2] (IR) and Raman-scattering[2,4] techniques. The original comparison of the Raman-active modes in SnO_2 and TiO_2 was made by Beattie and Gilson[3]; subsequent investigations were made by Scott[4] and Katiyar *et al.*[2] These last authors measured the absorption and reflection IR spectra as well as the Raman spectra. Using these data and assuming a rigid-ion model, they calculated the elastic constants and phonon-dispersion curves for SnO_2.

Anharmonic interactions among the phonons are known to be important in the lattice dynamics for this structure and result in temperature-dependent frequencies for the normal modes. In rutile, detailed measurements have shown that anharmonicities produce (i) large values and large temperature[5] and pressure[5,6] dependences of the static dielectric constants, (ii) strong temperature dependence of the long-wavelength A_{2u} phonon frequency,[7] and (iii) anomalous temperature and pressure dependences of the long-wavelength B_{1g} phonon frequency.[6,8] Measurements of both the temperature and pressure dependences of the individual phonon frequencies allow one to distinguish the pure-volume and pure-temperature contributions to the

self-energy.[9,10] Such measurements have been performed in rutile in which anomalous temperature and pressure dependences for various modes were found. It is of interest, therefore, to perform a corresponding analysis on SnO_2 to examine the generality of the conclusions inferred from the measurements on rutile and to determine if they are characteristic of this type of structure.

The purpose of this paper is to present the temperature and pressure dependences of the Raman-active-phonon frequencies in SnO_2 and compare the results with TiO_2 wherever applicable. First the experimental details (Sec. II) and the crystal structure (Sec. III) are discussed. The results are presented and discussed in Sec. IV and summarized in Sec. V.

II. EXPERIMENTAL ARRANGEMENT

The Raman spectra were obtained with ~150-mW incident power at either 5145 or 4880Å. All data were taken in a right-angle scattering geometry. The sample used in these measurements was a small (~1×1×3 mm) synthetically grown single crystal kindly furnished by Tunheim. The crystal was of good optical quality, but contained ~ 50 ppm Fe impurities which produced weak fluorescence near 4880 Å. As a result, detailed measurements of the temperature dependence of the Raman spectra were made using both 4880- and 5145-Å excitation.

In view of the questions which exist in the literature concerning the B_{1g} mode, further details about the sample geometry are in order. Our small
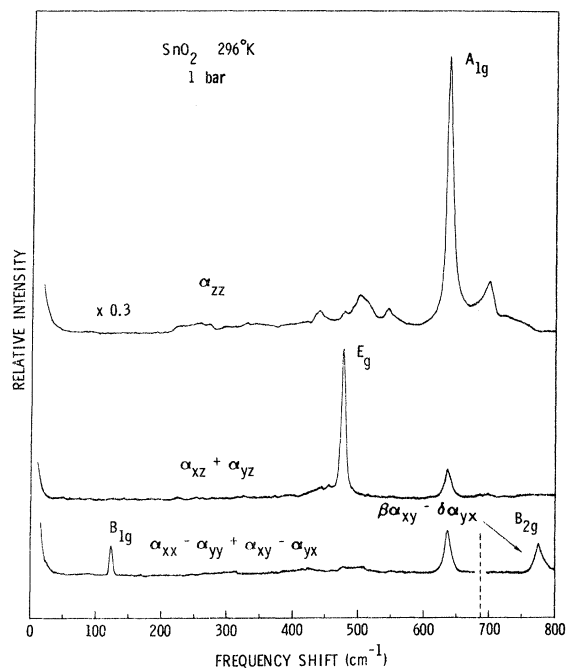
FIG. 1. Raman spectra illustrating the four Raman-active modes for SnO$_2$. The B_{2g} mode is obtained by rotating the sample $\sim 10°$ to prevent complete cancellation of the xy-yx contribution for the polarizability tensor.

crystal possessed (110) faces along the 1-mm dimensions with the c axis along the longer dimension. Inability to prepare optical surfaces normal to the a and c axes prevented suitable polarization measurements for complete separation of the various modes. However, a simple transformation from the laboratory x', y', and z' axes to the crystal x, y, and z axes allows detailed examination of the selection rules. Data showing the Raman spectra for the various modes at room temperature are given in Fig. 1. The observation of the B_{1g} mode will be discussed in more detail in Sec. IV F.

For temperatures below 296 °K, the samples was mounted in a variable-temperature Dewar and cooled by the boiloff from liquid helium. The temperature was stabilized to ± 0.1 °K and monitored at the sample block with a Ge resistance thermometer for $T \lesssim 50$ °K and a Pt resistance thermometer for $T \gtrsim 50$ °K. For $T > 296$ °K, the sample was mounted in an oven and the temperature monitored with an iron-constantan thermocouple.

The pressure cell used in these experiments was similar to that described by Brafman et $al.$[11] The cell was made of nickel maraging steel and had three windows of fused silica to allow a 90 ° scattering geometry. The sample was immersed in the pressure fluid (Isopar H, Humble Oil Co.) to ensure a completely hydrostatic environment. Pressure was measured to ± 20 lb/in.^{2} with a

Heise Bourdon-tube gauge calibrated against a dead-weight gauge.

To measure the pressure dependence of the lattice constants, a crystal specimen from this sample was mounted in a beryllium high-pressure cell[12] and high-purity dehydrated kerosene was used as the pressure fluid. This cell allowed x-ray-diffraction measurements over large diffraction angles (0 ° $\leq 2\theta \leq 165$ °), ensuring accurate determinations of the lattice constants. The lattice constants were determined up to 3 kbar by measuring ten Bragg peaks with 2θ values in the range 140 ° – 165 ° using Cu $K\alpha$ radiation ($\lambda_{K\alpha} = 1.54050$ Å). The values of the a and c axes were then determined by a least-squares fit to the data.

The thermal expansion was measured from 93 to 700 °K using the same Bragg peaks as were used in the pressure measurements. For temperatures below 296 °K, the sample was cooled with flowing N_2 gas and for temperatures above 296 °K, the sample was mounted in a high-temperature x-ray-diffraction furnace.[13] In addition, the room-temperature lattice parameters were determined from a powdered sample prepared from the same material. The Debye–Scherrer pattern yielded the lattice parameters $a = 4.7348(2)$ Å and $c = 3.1862(1)$ Å, in good agreement with previous values ($a = 4.73727$ Å and $c = 3.186383$ Å).[14]

III. CRYSTAL STRUCTURE AND RAMAN-ACTIVE PHONONS

Cassiterite has the tetragonal rutile structure (space group D_{4h}^{14}, $P4/mnm$) with two SnO$_2$ molecules per unit cell. The irreducible representation of the optic modes is

$$\Gamma = A_{1g} + A_{2g} + B_{1g} + B_{2g} + E_g + A_{2u} + 2B_{1u} + 3E_u. \quad (1)$$

Modes of symmetry A_{2g} and B_{1u} are optically inactive, while modes of symmetry A_{2u} and E_u are IR active. The remaining optic modes, A_{1g}, B_{1g}, B_{2g}, and E_g, are Raman active in first order with the polarizability tensors

$$\alpha(A_{1g}) = \begin{pmatrix} a & 0 & 0 \\ 0 & a & 0 \\ 0 & 0 & b \end{pmatrix}, \quad \alpha(B_{1g}) = \begin{pmatrix} c & 0 & 0 \\ 0 & -c & 0 \\ 0 & 0 & 0 \end{pmatrix},$$

$$\alpha(B_{2g}) = \begin{pmatrix} 0 & f & 0 \\ f & 0 & 0 \\ 0 & 0 & 0 \end{pmatrix}, \quad \alpha(E_g) = \begin{pmatrix} 0 & 0 & d \\ 0 & 0 & d \\ d & d & 0 \end{pmatrix}. \quad (2)$$

Only these four modes were measured in the present experiments. Their $q \approx 0$ displacements are shown in Fig. 2. The frequencies of the Raman-active modes are compared with the corresponding frequencies of TiO$_2$ in Table I; also included in Table I are the frequencies of these modes determined from previous measurements.
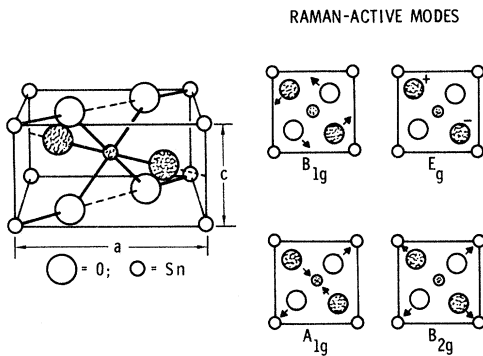
RAMAN-ACTIVE MODES

FIG. 2. Structure of SnO_2 and $q \approx 0$ displacements, viewed along the c axis, for the Raman-active modes.

IV. RESULTS AND DISCUSSION

A. Isothermal Compressibility and Thermal Expansion

The pressure dependence of the lattice constants and the c/a ratio for SnO_2 are shown in Fig. 3. The decreases are linear over the pressure range covered, and the measured isothermal compressibilities are $\kappa_a \equiv -(\partial \ln a/\partial P)_T = 1.3 \times 10^{-4}$/kbar and $\kappa_c \equiv -(\partial \ln c/\partial P)_T = 1.9 \times 10^{-4}$/kbar; thus $\kappa \equiv (\partial \ln V/\partial P)_T = 2\kappa_a + \kappa_c = 4.5 \times 10^{-4}$/kbar for SnO_2. This volume compressibility for SnO_2 is smaller than that for TiO_2, which is 4.73×10^{-4}/kbar. Note that κ_c for SnO_2 is greater than κ_a, while for TiO_2 the opposite is true.
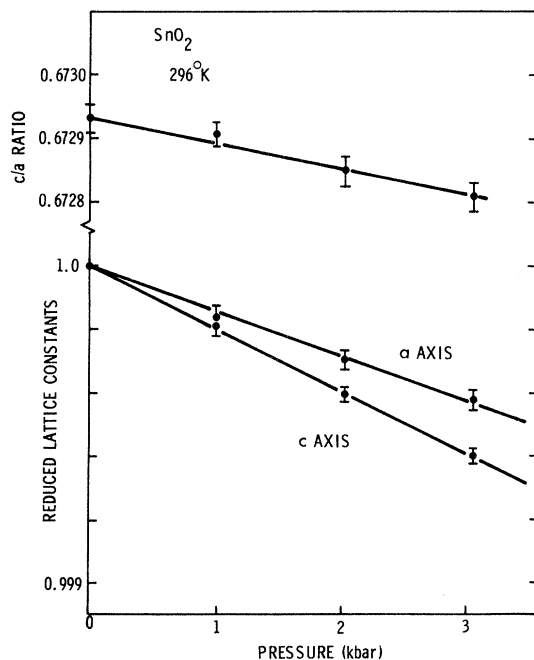
Figure 4 shows the temperature dependence of

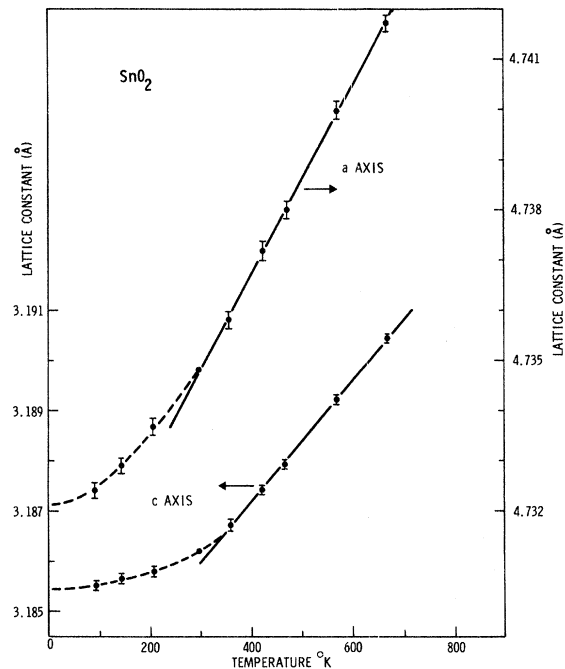FIG. 3. Reduced lattice parameters and change in c/a with hydrostatic pressure for SnO_2 at 296 °K.

FIG. 4. Lattice constants as a function of temperature for SnO_2.

the lattice constants. The thermal expansivities are linear for $T \gtrsim 350$ °K. In the high-temperature region, the thermal expansion coefficients are β_a

TABLE I. Frequencies of the Raman-active phonons in SnO_2 compared to the corresponding modes in TiO_2.

SnO_2	ω (cm^{-1})	T (°K)	TiO_2	T (°K)
B_{1g}	121[a]	10	142[b]	10
	123[a]	296	143	296
	87[c]	~296		
E_g	476[a]	10	455[b]	10
	475[a]	296	450[b]	296
	472[c]	296		
	476[d]	100		
	476[e]	296		
A_{1g}	637[a]	10	611[b]	10
	634[a]	296	612[b]	296
	632[c]	296		
	638[d]	100		
	634[e]	296		
B_{2g}	781[a]	10		
	776[a]	296	826[b]	296
	773[c]	296		
	782[d]	100		
	778[e]	296		

[a]This work; only these measurements were made on a synthetic crystal, while the measurements in Refs. 2–4 were made on natural cassiterite.
[b]Reference 6.
[c]Reference 4.
[d]Reference 2 (B_{1g} not observed).
[e]Reference 3 (B_{1g} not observed).

TABLE II. Compressibilities and thermal expansivities of SnO_2 and TiO_2.

		κ (296 °K) (10^{-4}/kbar)	β ($T > 350$ °K) (10^{-6}/°K)
a axis	SnO_2	1.3	4.0
	TiO_2	1.93	8.5
c axis	SnO_2	1.9	3.7
	TiO_2	0.87	11.0
volume	SnO_2	4.5	11.7
	TiO_2	4.73	28.0

$= (\partial \ln a/\partial T)_P = 4.0 \times 10^{-6}/°K$ and $\beta_c = (\partial \ln c/\partial T)_P = 3.7 \times 10^{-6}/°K$. Again, the ratio β_a/β_c is reversed from that for TiO_2 which has $\beta_a = 8.5 \times 10^{-6}/°K$ and $\beta_c = 11.0 \times 10^{-6}/°K$ at high temperatures. The volume expansion coefficient for SnO_2 is $\beta \equiv (\partial \ln V/\partial T)_P = 2\beta_a + \beta_c = 11.7 \times 10^{-6}/°K$, which is much smaller than the value of $28.0 \times 10^{-6}/°K$ for TiO_2. These results are summarized in Table II.

Even though TiO_2 and SnO_2 belong to the same structure type, a comparison of the above-mentioned linear compressibilities and expansivities suggests an important difference. Namely, with changes in either temperature or pressure, the structures deform in opposite directions. This "antiparallel" behavior appears to be important in relation to the pressure-induced transitions which occur in these materials. We shall elaborate on this in Sec. IV F.
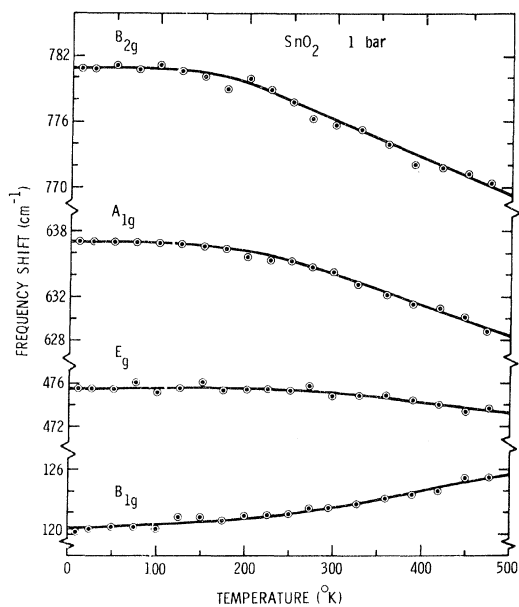
FIG. 5. Temperature dependence of the frequencies of the Raman-active modes in SnO_2.

B. Temperature and Pressure Dependence of Phonon Frequencies

Figure 5 shows the variation of the frequencies of the four Raman-active modes with temperature T at 1 bar from 10 to 500 °K. The modes E_g, A_{1g}, and B_{2g} exhibit normal T dependences, in that their frequencies decrease with increasing T, while B_{1g} is anomalous, with $\omega(B_{1g})$ increasing with increasing T. A similar T dependence was observed in TiO_2,[6] although the change in TiO_2 was much smaller than in SnO_2 $\{[\partial \ln\omega(B_{1g})/dT]_P = +0.6 \times 10^{-5}/°K$ for TiO_2 compared with $+11.9 \times 10^{-5}/°K$ for $SnO_2\}$. The temperature derivatives $(\partial \ln\omega_i/\partial T)_P$ for SnO_2 are summarized in Table III. These values represent the high-T region, where the frequencies all vary approximately linearly with T and the logarithmic slope is obtained from a least-squares fit to the data assuming a linear T variation.

Also included in Table III are the logarithmic pressure (P) derivatives of the Raman-active frequencies in SnO_2 at 296 °K. The pressure results are given in Fig. 6. The P dependences of the E_g, A_{1g}, and B_{2g} modes are normal—i.e., $(\partial \ln\omega_i/\partial P)_T$ positive-as were the T dependences; again, mode B_{1g} is anomalous in that $[\partial \ln\omega(B_{1g})/\partial P]_T$ is negative, similar to the B_{1g} mode of TiO_2.[6,8] The implications of the anomalous temperature and pressure dependences will be discussed in more detail in Sec. IV F.

C. Explicit Volume and Temperature Dependences of the Raman-Active Modes

The variations of the frequencies of the optic modes with temperature at constant pressure are composed of two contributions: (i) changes which arise from the change in volume with temperature and (ii) the explicit temperature dependence at constant volume. Treating ω_i as a function of the volume V and temperature T yields

$$\left(\frac{\partial \ln\omega_i}{\partial T}\right)_P = \left(\frac{\partial \ln V}{\partial T}\right)_P \left(\frac{\partial \ln\omega_i}{\partial \ln V}\right)_T + \left(\frac{\partial \ln\omega_i}{\partial T}\right)_V$$

$$= -\frac{\beta}{\kappa}\left(\frac{\partial \ln\omega_i}{\partial P}\right)_T + \left(\frac{\partial \ln\omega_i}{\partial T}\right)_V . \tag{3}$$

TABLE III. Frequencies of the Raman-active phonons of SnO_2 and their logarithmic pressure and temperature derivatives with the isobaric temperature derivatives separated into pure-volume and pure-temperature contributions at 296 °K.

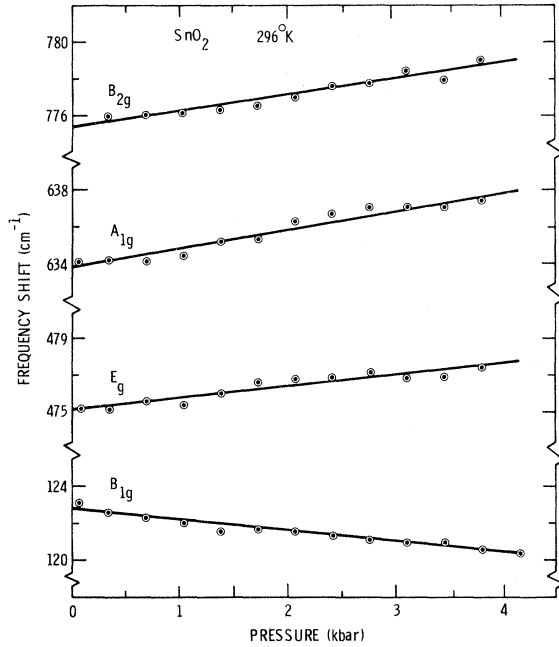| Mode	ω (cm^{-1})	$\left(\frac{\partial \ln \omega}{\partial P}\right)_T$ (10^{-3}/kbar)	$\left(\frac{\partial \ln \omega}{\partial T}\right)_P$ (10^{-5}/°K)	$= -\frac{\beta}{\kappa}\left(\frac{\partial \ln \omega}{\partial P}\right)_T$ (10^{-5}/°K)	$+\left(\frac{\partial \ln \omega}{\partial T}\right)_V$ (10^{-5}/°K)
B_{1g}	123	-4.7 ± 0.2	$+12.5 \pm 0.5$	9.8	2.7
E_g	475	1.3 ± 0.2	-1.8 ± 0.5	-3.0	1.2
A_{1g}	634	1.6 ± 0.2	-4.3 ± 0.5	-3.4	-0.9
B_{2g}	776	1.2 ± 0.2	-4.4 ± 0.5	-2.4	-2.0

FIG. 6. Pressure dependences of the frequencies of the Raman-active modes in SnO_2.

The first term on the right-hand side of Eq. (3) is the pure-volume contribution to the isobaric temperature dependence of ω_i, and the second term is the pure-temperature contribution. Equation (3) is strictly true only for cubic crystals. For the present tetragonal system, there could also be a contribution from the change in c/a with temperature or pressure; however, the relative change in c/a is approximately an order of magnitude less than the relative volume change with either temperature or pressure (Sec. IV A). We therefore have neglected changes in c/a relative to the changes in volume. The data presented in Secs. IV A and IV B thus allow an evaluation of the pure-volume and pure-temperature contributions to ω_i. These results at 296 °K are presented in Table III.

From Table III it is seen that the magnitude of the pure-volume contribution to the isobaric temperature dependence dominates the pure-temperature contribution for each of the modes investigated with the exception of $\omega(B_{2g})$. In TiO_2, the pure-temperature and pure-volume contributions to $\omega(B_{1g})$ were comparable in magnitude and opposite in sign, whereas for SnO_2 the isobaric frequency shift of B_{1g} is dominated by the pure-volume contribution.

D. Mode Grüneisen Parameters

The mode Grüneisen parameters γ_i are defined by

$$\gamma_i \equiv -\left(\frac{\partial \ln\omega_i}{\partial \ln V}\right)_T = \frac{1}{\kappa}\left(\frac{\partial \ln\omega_i}{\partial P}\right)_T . \qquad (4)$$

The data shown in Fig. 6 and presented in Table III, along with the value of κ, are sufficient to determine γ_i for each Raman-active mode at 296 °K. The values for γ_i are compared with those of TiO_2 in Table IV. All modes except B_{1g} exhibit typical γ_i for normal ionic crystals; the anomalous behavior of B_{1g} is evident from the large negative value of -10.44 for $\gamma(B_{1g})$. This behavior is similar to the B_{1g} mode in TiO_2, where $\gamma(B_{1g}) = -5.03$. The B_{1g} mode is further discussed below.

E. Anharmonic Interactions

Anharmonic interactions among the phonons produce temperature-dependent phonon frequencies through two separate contributions: (i) a pure-volume contribution which results from thermal expansion and (ii) a pure-temperature contribution which results from cubic and quartic anharmonicities. Such a contribution has been calculated by Maradudin and Fein[15] and Cowley.[9] The calculations are very complex and only qualitative evaluation of the origins of the anharmonicities can be made. In view of this, only a schematic presentation of the results are given.

The frequency of the jth mode at wave vector q is given by Cowley[9] as

$$\omega^2(qj) = \omega_0^2(qj) + 2\omega_0(qj)D(qjj', \Omega), \qquad (5)$$

where $\omega_0(qj)$ is the harmonic frequency and $D(qjj', \Omega)$ is the anharmonic contribution to the self-energy of the mode. The frequency Ω depends on the measurement technique[9]; for these measurements, $\Omega \sim \omega(qj)$. The anharmonic term D (we drop all subscripts for simplicity) contributes both a frequency shift Δ and damping Γ to the phonon modes, resulting in $D = \Delta - i\Gamma$.

Schematically, Δ is given to lowest order in perturbation theory by

$$\Delta = \Delta^E + \Delta_3 + \Delta_4 \equiv \Delta^E + \Delta^A , \qquad (6)$$

where Δ^E represents the anharmonic frequency shift due to thermal expansion, Δ_3 the frequency shift due to cubic anharmonicities, and Δ_4 the fre-

TABLE IV. Mode frequencies and Grüneisen parameters for SnO_2 compared to those of TiO_2.

Mode	$\omega(SnO_2)$ (cm^{-1})	$\gamma(SnO_2)$	$\omega(TiO_2)^a$ (cm^{-1})	$\gamma(TiO_2)^a$
B_{1g}	123	-10.44	143	-5.03
E_g	475	3.20	450	2.43
A_{1g}	634	3.64	612	1.59
B_{2g}	776	2.58	826	...

^{a}Reference 6.

quency shift due to quartic anharmonicities. Δ_3 results from the cubic interaction taken to second order, and Δ_4 is the first-order term in the quartic interaction. The combined contribution $\Delta_3 + \Delta_4$ is the pure-temperature contribution to the isobaric temperature dependence of the frequencies. Furthermore, Δ_3 is negative definite for small Ω, while Δ_4 can be either positive or negative, which, in some cases, allows one to distinguish the origin of the anharmonicities.

As indicated previously, the measurements of $\omega_i(T)$ and $\omega_i(P)$ permit a separate determination of Δ^E and $\Delta_3 + \Delta_4$. Rewriting Eq. (3)

$$(\Delta\omega_T)_P = - (\Delta\omega_P)_T + (\Delta\omega_T)_V , \tag{7}$$

where $(\Delta\omega_T)_P$ is the change in ω on raising T from 0 to $T\,°K$ at constant pressure (1 bar), $(\Delta\omega_T)_V$ is the change in ω on raising T from 0 to $T\,°K$ at constant volume (the volume at $T = 0\,°K$, $P = 1$ bar), and $- (\Delta\omega_P)_T$ is the change in ω on raising P at constant T from 1 bar to a value of P sufficient to decrease V from its value at $T\,°K$ at $P = 1$ bar to its value at $0\,°K$ at $P = 1$ bar. The quantities $(\Delta\omega_P)_T$ and $(\Delta\omega_T)_V$ can be obtained from β, $\omega_i(T)$, and the Grüneisen parameters γ_i. The mode Grüneisen parameters (Sec. IV D) were determined only at 296 °K; however, they are known to be relatively temperature independent for this crystal class. A linear decrease in the γ_i's of 2%/100 °K, typical for this class of crystals, will be assumed for evaluation of the T dependence of pure-temperature and pure-volume contributions to the phonon self-energies. Substantial error in the assumed value of $d\gamma_i/dT$ will not significantly affect our conclusions. The variations of $(\Delta\omega_P)_T$ and $(\Delta\omega_T)_V$ are given in Fig. 7 for T from 0 to 500 °K. A very interesting feature of these results is that the pure-volume contribution dominates the pure-temperature contribution throughout the entire temperature range investigated except for mode B_{2g}, where they are comparable. The volume contribution, which results from thermal expansion, is simply $\Delta^E = - (\Delta\omega_P)_T$. The pure-temperature contribution, which results from higher-order anharmonicities, is given by[10]

$$(\Delta\omega_T)_V \cong \Delta_T^A - \Delta_0^A . \tag{8}$$

In Eq. (8), Δ_0^A is the anharmonic contribution to the phonon energy associated with zero-point motion, and Δ_T^A is the T-dependent contribution of the higher-order anharmonicities $\Delta_3 + \Delta_4$. In the high-T limit, the volume, the phonon occupation numbers, and $(\Delta\omega_T)_V$ increase linearly with T; therefore, an estimate of $- \Delta_0^A$ is obtained from an extrapolation of the linear region of $(\Delta\omega_T)_V$ back to $0\,°K$. Although the linear approximation is rigorously valid only at $T > \theta_D$, the phonon frequencies and the thermal expansivities are observed to be lin-

ear for $T \gtrsim 300\,°K$. Extrapolation of the high-T linear region of $(\Delta\omega_T)_V$ to $0\,°K$ reveals that $|-\Delta_0^A| < 1$ cm^{-1} for all modes, and is therefore $< 1\%$ of the phonon energies in all cases. In fact, the higher-order anharmonicities Δ^A contribute less than 1% of the phonon energies at all T.

As mentioned previously, cubic anharmonicities Δ_3 lead to negative frequency shifts for small Ω, while the quartic anharmonicities Δ_4 may contain either positive or negative contributions to the phonon frequencies. In the cases of the A_{1g} and B_{2g} modes, Δ^A is negative, so that the anharmonicities may be due either to cubic or to quartic interactions. On the other hand, Δ^A is positive for both B_{1g} and E_g, indicating that Δ^A is dominated by positive quartic anharmonicity for these two modes.

The results in this section quantitatively show that the self-energy shifts are small for modes B_{1g}, E_g, A_{1g}, and B_{2g}, so that the mode frequencies are dominated by the quasinormal frequencies ω_0. The Raman-active modes of SnO_2 are similar to the corresponding modes of TiO_2 in this respect; however, for all modes, the anharmonic self-energy shifts are smaller in SnO_2 than in TiO_2. The isobaric T dependences of $\omega(B_{1g})$, $\omega(E_g)$, and $\omega(A_{1g})$ are dominated by the thermal expansion Δ^E, while the T dependence of $\omega(B_{2g})$ results about equally from thermal expansion and higher-order anharmonicities.
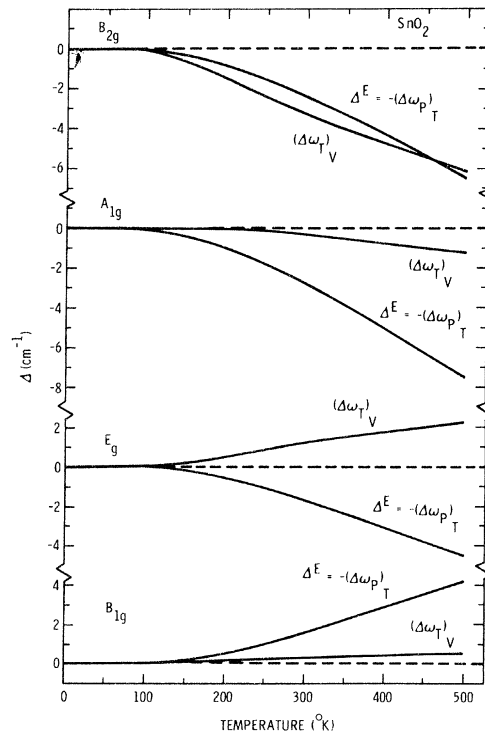

FIG. 7. Self-energies of the Raman-active modes of SnO_2 versus temperature.

TABLE V. Transition pressures and high-temperature logarithmic pressure and temperature derivatives of c/a and the pressure dependences of $\omega(B_{1g})$ for four crystals of the rutile structure.

Crystal	$\omega(B_{1g})$ (cm^{-1})	$\left(\dfrac{\partial \ln\omega(B_{1g})}{\partial P}\right)_T$ (10^{-3}/kbar)	$\left(\dfrac{\partial \ln(c/a)}{\partial T}\right)_P$ (10^{-6}/°K)	$\left(\dfrac{\partial \ln(c/a)}{\partial P}\right)_T$ (10^{-4}/kbar)	P_{trans} (kbar)
SnO$_2$	123	-4.7	-0.25	$+0.6$	~ 250[a]
NiF$_2$	72[b]	-5.4[b,h]	-3.7[c]	...	~ 130[d]
TiO$_2$	143[e]	-2.4[e]	$+2.5$[e]	-1.0[e]	~ 26[f], ~ 200[g]
MnF$_2$ II–III	60[b]	$-14.$[b,h]	$+9.2$[i]	-2.7[j]	~ 33[d]
					~ 150[d]

[a]Reference 18. [c]Reference 20. [e]Reference 6. [g]Reference 16. [i]Reference 22.
[b]Reference 19. [d]Reference 21. [f]Reference 8. [h]Preliminary results. [j]Reference 23.

F. B_{1g} Mode

The anomalous behavior of the B_{1g} mode in both SnO$_2$ and TiO$_2$ has been stressed throughout this discussion. Before dealing with the lattice-dynamical implications of the pressure and temperature dependence of $\omega(B_{1g})$ in SnO$_2$, it should be noted that the present measurements apparently constitute the first observation of this mode in SnO$_2$. In the original measurements of Raman scattering from SnO$_2$, Beattie and Gilson[3] did not observe $\omega(B_{1g})$, and estimated its intensity $I(B_{1g})$ to be $< 10^{-2} I(A_{1g})$. Subsequently, Scott[4] observed a mode at 87 cm^{-1}, which was attributed to B_{1g}, while we attribute the mode at 123 cm^{-1} (296 °K) to B_{1g}. It should be noted, however, that the crystal used in Scott's measurements was natural cassiterite of poor optical quality and contained sufficient impurities to color it. The frequencies of the remaining modes agree well with the values reported here. Finally, the detailed measurements of Katiyar et al.[2] also failed to reveal the B_{1g} mode. The authors estimate $I(B_{1g}) < 10^{-3} I(A_{1g})$. Comparison of $I(B_{1g})$ and $I(A_{1g})$ in our sample yields $I(B_{1g})/I(A_{1g}) \sim 3 \times 10^{-3}$, which presumably should have been observable if $I(B_{1g})/I(A_{1g})$ is sample independent. Support for our assignment of the 123-cm^{-1} mode as B_{1g} is also given by the similarity between the pressure and temperature dependences of its frequency and the corresponding dependences of $\omega(B_{1g})$ in TiO$_2$. The two essential differences between our measurements and previous measurements are that we used synthetically grown SnO$_2$, whereas the other measurements were made on naturally occurring cassiterite; furthermore, B_{1g} was measured in a geometry which gave the sum of the two polarizability components. The agreement among the various measurements for $\omega(A_{1g})$, $\omega(E_g)$, and $\omega(B_{2g})$ is remarkable (Table I), but the discrepancies for $\omega(B_{1g})$ are not understood. We further note that the measured $\omega(B_{1g})$ is $\sim 20\%$ greater than the value of 100 cm^{-1} calculated by Katiyar et al.[2] on the basis of a rigid-ion model.

From the negative pressure dependence of $\omega(B_{1g})$, it is probable that this mode plays an important role in the pressure-induced phase transitions which occur in this crystal class. An examination of the available experimental data which are of importance in the pressure-induced transitions is revealing. Table V summarizes the data for the isomorphous compounds SnO$_2$, TiO$_2$, MnF$_2$, and NiF$_2$. These four crystals were chosen for this comparison, since they are the only members of this crystal class for which the pressure dependence of $\omega(B_{1g})$ has been measured. In all cases, the transition pressures given are only approximate, and the crystal structures of the high-pressure phases are not known. Furthermore, MnF$_2$ exhibits two pressure-induced transitions, and in the case of TiO$_2$ Nicol and Fong[8] reported a transition at ~ 26 kbar in an apparatus where nonhydrostatic strains can be substantial, whereas other workers[16] have seen evidence for a transition at ~ 200 kbar. It is not known if the two high-pressure phases are identical. It has been suggested that the high-pressure phase(s) of TiO$_2$ are either orthorhombic α-PbO$_2$[8] or orthorhombic CaCl$_2$.[17]

The axial compressibilities and thermal expansivities allow us to separate the four compounds listed above into two groups as shown in Table V. While $\omega(B_{1g})$ decreases with pressure for all four compounds, the different behavior of c/a with temperature and pressure, emphasized by the grouping in Table V, may be of importance in determining the nature of the pressure-induced phase transition. The following observations can be made from these data: (i) The c/a ratio decreases with increasing temperature for SnO$_2$ and NiF$_2$, but increases for TiO$_2$ and MnF$_2$. (ii) The c/a ratio increases with increasing pressure for SnO$_2$ (no data available for NiF$_2$), but decreases for TiO$_2$ and MnF$_2$. (iii) $\omega(B_{1g})$ decreases with increasing pressure and increases with increasing temperature (not shown) for all four compounds. In view of the fact that the $P(V)$ relationships do not show much curvature, the initial pressure derivatives

of $\omega(B_{1g})$ can be extrapolated to the transition pressure. For SnO_2 and NiF_2 these initial pressure derivatives yield $\omega(B_{1g}) \to 0$ at pressures very close to the observed transition pressures. On the other hand, for TiO_2 and MnF_2 extrapolation of the low-pressure data suggests that $\omega(B_{1g}) \to 0$ at pressures much higher than the observed transition pressure. If the phase transitions in these crystals are driven by the softening of the B_{1g} mode with pressure, then the transitions in SnO_2 and NiF_2 may be close to second order, whereas those in TiO_2 and MnF_2 are strongly first order, since ω need not vanish at a first-order transition.

While these considerations must be considered speculative until more information concerning the high-pressure phases of these materials is obtained, it seems that both the B_{1g} mode and the axial compressibilities play fundamental roles in the pressure-induced transitions in crystals of the rutile structure. A detailed understanding of the pressure-induced transitions will require either more measurements at higher pressures or calculations which include the effects of the optic modes and axial compressibilities.

V. CONCLUSIONS

Detailed measurements of the pressure and tem-
perature dependences of the Raman-active phonons A_{1g}, B_{1g}, E_g, and B_{2g} were combined with measurements of the thermal expansivity and compressibility to determine the pure-volume and pure-temperature contributions to the isobaric temperature dependences of these modes of SnO_2. These measurements show that the anharmonic contributions to the phonon self-energies are $< 1\%$ of the harmonic contribution. Furthermore, the anharmonic self-energy shifts are dominated by the thermal expansion for all modes except B_{2g}, where the thermal expansion and higher-order anharmonicities contribute about equally. The decrease in $\omega(B_{1g})$ with pressure yields a large negative mode Grüneisen parameter $[(\gamma B_{1g}) = -10.4]$, and the implications of this behavior relative to the pressure-induced phase transition in SnO_2 are discussed.

†Work supported by the U. S. Atomic Energy Commission.

[1]R. Summitt and N. F. Borrelli, J. Phys. Chem. Solids 26, 921 (1965).

[2]R. S. Katiyar, P. Dawson, M. M. Hargreave, and G. R. Wilkinson, J. Phys. C 4, 2421 (1971).

[3]I. R. Beattie and T. R. Gilson, Proc. R. Soc. A 307, 407 (1968).

[4]J. F. Scott, J. Chem. Phys. 53, 852 (1970).

[5]R. A. Parker, Phys. Rev. 124, 1719 (1961).

[6]G. A. Samara and P. S. Peercy, Phys. Rev. (to be published).

[7]J. G. Traylor, H. G. Smith, R. M. Nicklow, and M. K. Wilkinson, Phys. Rev. B 3, 3457 (1971).

[8]M. Nicol and M. Y. Fong, J. Chem. Phys. 54, 3167 (1971).

[9]R. A. Cowley, Philos. Mag. 11, 673 (1965); Adv. Phys. 12, 421 (1963).

[10]R. P. Lowndes, J. Phys. C 4, 3083 (1971).

[11]O. Brafman, S. S. Mitra, R. K. Crawford, W. B. Daniels, C. Postmus, and J. R. Ferraro, Solid State Commun. 7, 449 (1969).

[12]B. Morosin and J. E. Schirber, Phys. Lett. A 30, 512 (1969).

[13]R. W. Lynch and B. Morosin, J. Appl. Crystallogr. 4, 352 (1971).

[14]R. W. G. Wyckoff, Crystal Structures (Interscience, New York, 1965), Vol. 1, p. 251.

[15]A. A. Maradudin and A. E. Fein, Phys. Rev. 128, 2589 (1962).

[16]R. K. Linde and P. S. DeCarli, J. Chem. Phys. 50, 319 (1969); J. C. Jamieson and B. Olinger, Science 161, 893 (1968).

[17]L. Nagel and M. O'Keefe, Mater. Res. Bull. 6, 1317 (1971).

[18]H. G. Drickamer, R. W. Lynch, R. L. Clendenen, and E. A. Perez-Albverne, in Solid State Physics, edited by F. Seitz and D. Turnbull (Academic, New York, 1966), Vol. 19, p. 135.

[19]P. S. Peercy (unpublished).

[20]K. V. K. Rao, S. V. N. Naida, and L. Iyengar, Indian J. Phys. 42, 622 (1968).

[21]S. S. Kabalkina, L. F. Vereshchagin, and L. M. Lityagina, Fiz. Tverd. Tela 11, 1040 (1969) [Sov. Phys.-Solid State 11, 847 (1969)].

[22]D. F. Gibbons, Phys. Rev. 115, 1194 (1959).

[23]R. L. Melcher, Phys. Rev. B 2, 733 (1970).